Journal of the Korean Ceramic Society
https://doi.org/10.1007/s43207-021-00184-8

ORIGINAL ARTICLE

Effect of boron nitride (BN) on mechanical and dielectric properties of fused silica ceramic composites

Kishore Kumar Kandi[1] · Gurabvaiah Punugupati[2] · Pagidi Madhukar[2] · C. S. P. Rao[2]

Received: 9 October 2021 / Revised: 24 December 2021 / Accepted: 27 December 2021

Abstract

In the current study, response surface methodology (RSM) was successfully used to the method of preparation of fused silica (SiO_2) ceramic composites using gelcasting, a near net shape method. The effects of input parameters like solid loading (SL), monomer content (MC), ratio of monomer (RM), and additive boron nitride (BN) and on responses such as flexural strength (FS), porosity (Por.), and dielectric constant (DE) were studied. RSM with central composite face-centered design with 6 center points approach used for planning the tests. The relation between the input variables on the output was investigated and modeled. Three regression models were established using RSM related independent input variables to describe the FS, Por., and DE as the response. The uniqueness of the established model is examined using Analysis of Variance (ANOVA) at 95% confidence level. The numerical investigation of the results showed that in range studied, the three process variables have significant effect on the responses. The obtained mathematical models have high R^2 values (97.66% for FS, 98.45% for Por., and 94.34% for DE) show the good relation between the test and predicted data. The optimal estimates found using RSM was practically confirmed and was 66.30 MPa FS, 23.66% Por., and 4.307 DE acquired at 47.97% SL, 15 wt% MC, 3 RM, and 9.68 wt% BN, respectively.

✉ Pagidi Madhukar
pmadhu88@gmail.com

[1] Department of Mechanical Engineering, CVR College of Engineering, Hyderabad, India

[2] Department of Mechanical Engineering, National Institute of Technology, Tadepalligudem, Andhra Pradesh, India

Published online: 25 January 2022

Graphical abstract

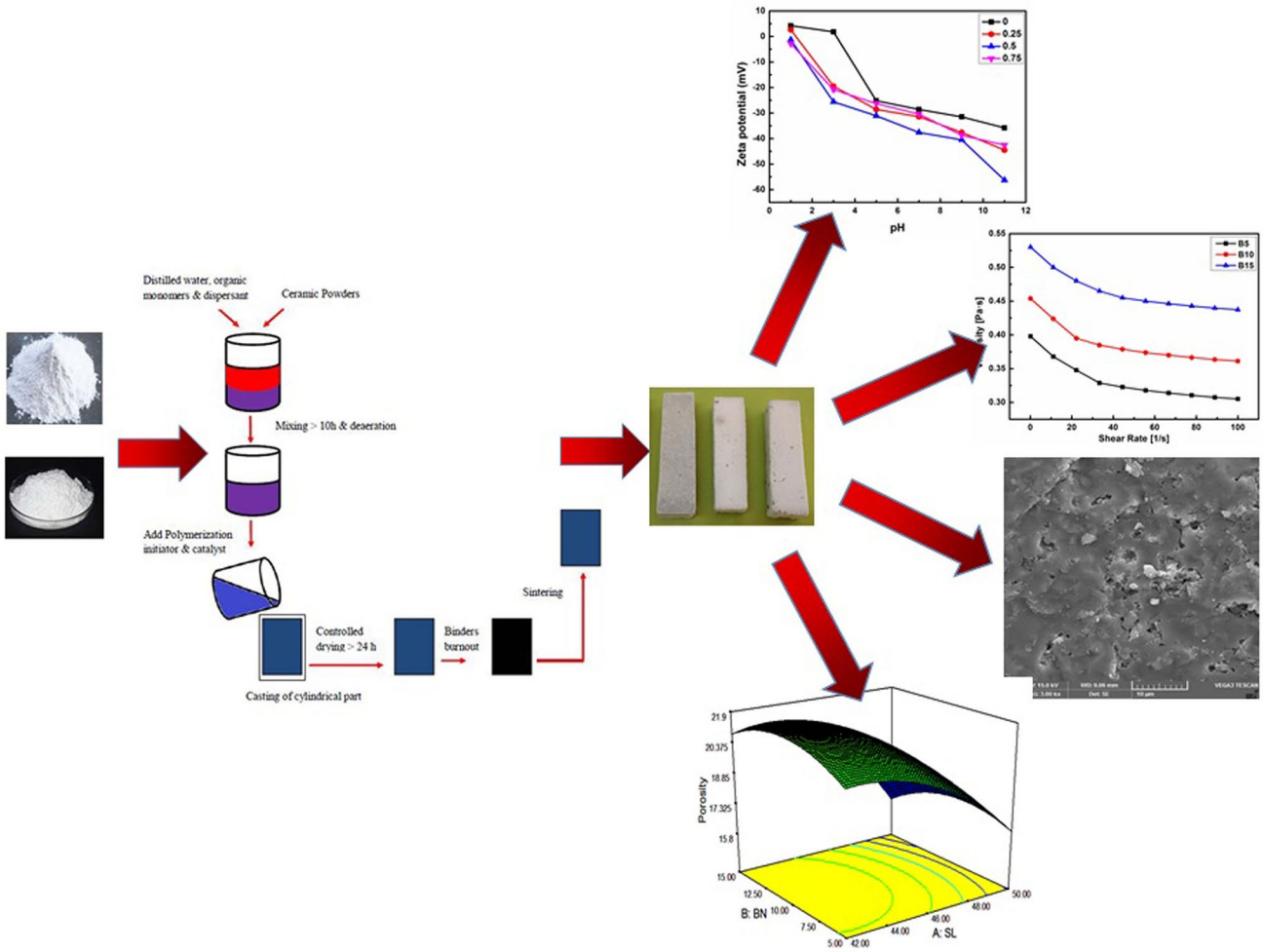

Keywords Fused silica · Boron nitride · Gelcasting · Flexural strength · Porosity · Dielectric constant · RSM

1 Introduction

Fused silica (SiO_2) is a non-crystalline solid, and consists of silicon dioxide which composes uneven connection between silicon and oxygen atoms forms non-crystalline structure through chemical bond which varies with the periodic network of crystal quartz. The amorphous structure is responsible for special mechanical, optical, physical, and chemical properties [1]. Fused SiO_2 ceramics possess low thermal expansion, high chemical resistance, excellent optical qualities, low DE, low loss tangent, and chemical properties. With exceptional physical and chemical properties, fused silica has various applications such as antenna windows, optical devices, heat shields, high power lasers, precision instruments, semiconductor manufacturing, aerospace applications, and these applications continuously increasing [2, 3]. The strength of the SiO_2 ceramics is somewhat low which is not sufficient to meet requirements of advanced hypersonic space craft applications. Therefore, to enhance these shortcomings reinforcements like Silicon Nitride (Si_3N_4) [4], Alumina (Al_2O_3) [5], Graphene [6], and Zirconia [7] were included as additives which gives improvement in the mechanical strength of the ceramics. These additives have better dielectric, mechanical, and chemical characteristics.

BN is a flexible material to facilitate in a number of applications owing to its distinctive combination of properties. Properties include better chemical inertness, thermal shock resistance, low thermal expansion, low DE and loss tangent, and high electrical resistance. This flexible material is currently used in a number of applications such as metal industry, automotive industry, high-temperature furnaces, etc. (Eichler and Lesniak) [8]. On the other hand,

the sinterability of BN ceramics is extremely poor and BN ceramics are normally manufactured by hot isostatic pressing or hot pressing at temperatures above 1800 °C, which is comparatively costly for their extensive use (Yuan et al.) [9]. Compared to Si_3N_4, BN has better thermal shock resistance and dielectric properties (Dong et al.) [10].

Wen et al. processed BN-SiO_2 composites by hot pressing of BN + SiO_2 powder blends ranging from 15 to 90 vol% BN, with a composition interval of 15 vol%. Plate-like grains of BN were conversely aligned by hot pressing and uniformly distributed in the SiO_2 matrix. The properties of SiO_2 such as FS and fracture toughness were significantly improved by 1.4 and 2.2 times with the addition of 15 vol% BN. The FS and fracture toughness at 60 vol% BN were found to be 246 MPa and 2.87 Mpa.$m^{1/2}$ [11]. Jia et al. prepared pressureless sintered 15 vol% BNp/SiO_2 composites by cold isostatic pressing (CIP) and gelcasting routes, respectively. Two types of SiO_2 powders with a particle size of 5.82 and 3.24 µm in d50, respectively, were used. The gelcasting pre-forming route has an awesome advantage above CIP route on the thermal stability of SiO_2 matrix. The maximum FS, fracture toughness, and Young's modulus were 101.5 ± 4.3 MPa, 1.57 ± 0.04 Mpa.$m^{1/2}$, and 61.3 ± 2.4 GPa, respectively [12]. Duan et al. prepared SiO_2 fiber-reinforced silica and BN-based composites (SiO_{2f}/SiO_2-BN) using the sol–gel technique and the urea route. Investigations were done on the microstructure, mechanical and dielectric properties, and the influence of oxidation process on the body. The FS, elastic modulus, density, DE, and loss tangent of SiO_{2f}/SiO_2-BN ceramic composites were 113.9 MPa, 36.5 GPa, 1.81 g/cm^3, 3.22 and 0.0039, respectively. The FS, elastic modulus, and density after oxidation treatment were decreased to 58.9 MPa, 9.4 GPa, and 1.80 g/cm^3. However, there is no significant effect of oxidation treatment on the dielectric properties of the composite [13]. Du et al. [14] employed two types of h-BN (BN nanotubes (BNNTs) and BN nanoparticles (BNNPs) to emphasize SiO_2 matrix consecutively to overwhelm intrinsic brittleness and meagre mechanical characteristics of SiO_2. Investigations were done on the mechanical and dielectric properties. The formation of cristobalite is controlled, and the fracture type and surface features were altered with the addition of BNNTs and BNNPs. Exceptional mechanical properties and low DE were demonstrated by 5 wt% BNNTs/SiO_2 and 5 wt% BNNPs/SiO_2 composites in contrast to monolithic SiO_2. The FS and fracture toughness were increased from 52.2 MPa and 0.58 MPa $m^{1/2}$ to 120.2 MPa and 1.22 Mpa $m^{1/2}$ by adding 7 wt% BNNPs [14]. Zhai et al. [15] prepared BN-SiO_2 composite ceramics by hot pressing sintering, using h-BN powder and SiO_2 sol as raw materials by varying SiO_2 from 10 to 40 wt%. The maximum FS obtained at 70 wt% h-BN was 180.30 MPa and a maximum fracture toughness of 3.20 MPa.$m^{1/2}$ was obtained at 80 wt% h-BN. The DE is in the range of 2.5–2.8 and the loss tangent with a magnitude of 10^{-3} (1 MHz to 2 GHz) was achieved [15].

RSM is defined as "a collection of mathematical and statistical techniques useful for the modeling and analysis of problems in which a response (output variable) of interest is influenced by several variables (input variables) and the goal is to optimize the responses that are influenced by the input process parameters" (Montgomery) [16]. Originally, RSM is developed to model experimental responses and then migrated into the modeling of numerical experiments (Box and Draper) [17]. They can be used for modeling and optimization of many engineering problems. Sufficient data are gathered through the experimental design layout and mathematical models for the desired responses as a function of selected variables were developed by applying the multiple regression analysis on the experimental data [18–21].

2 Materials and methods

Commercially available SiO_2 and BN (both M/s. Ants Ceramics Pvt. Ltd., Thane, India) with an average particle size of 1–5 µm are used in this study. Deionized water is used as a solvent. Commercially available dispersants such as Darvan 821A and Darvan C-N (both R.T Vanderbilt, Norwalk, CT), Dolapix A88, and Dolapix CE64 (both Zschimmer & Schwarz, Lahnstein, Germany) are used for dispersing ceramic particles in slurries for obtaining high SL and low viscosity. In the method of gelcasting, Methacrylamide and *N,N′*- methylenebisacrylamide (both Alfa Aesar) are utilized as the organic monomer and cross-linker, respectively. Ammonium persulfate (APS) and *N,N,N′,N′*-Tetramethylethylenediamine (TEMED) (both Alfa Aesar, United Kingdom) are used as the initiator and catalyst. Surface exfoliation phenomenon of green samples cast in the air was removed by adding Polyethylene glycol 400 (Alfa Aesar, United Kingdom). Diluted nitric acid and ammonium hydroxide (both S.D. fine chemicals, India) were utilized for pH adjustment.

3 Slurry preparation

SiO_2 and BN ceramic composites were fabricated using Gelcasting at different SL using different MC, RM, and BN contents. Initially, the premix solution was prepared by adding Darvan 821A dispersant (1 Wt% MC), PEG (surfactant), and monomers MAM and MBAM (Wt% of SiO_2) in distilled water. The solution was stirred with magnetic stirrer. The premix solution was added with solid loading of required vol% of fused silica and stirred more than 6 h. The entrapped air in the slurry was removed for 15–20 min

using deaerator, and then, initiator APS (1 wt% of MC) and TEMED were added for initiating polymerization and solidification.

Finally, the slurry was poured into a glass mold, and after polymerization, the green bodies were demolded. The green bodies were dried in a controlled humidity conditions for 24 h. The binders were burn out at 600 °C in a high-temperature muffle furnace for 1 h with a heating rate of 2 °C/min. The sintering process for ceramic samples was conducted in the nitrogen environment at 1250 °C with a heating rate of 4 °C/min. The detailed flowchart of gelcasting process for the preparation of any of the ceramic composite concern, i.e., SiO_2–BN, is shown in Fig. 1. A sintered sample of SiO_2–BN ceramic composite is shown in Fig. 2.

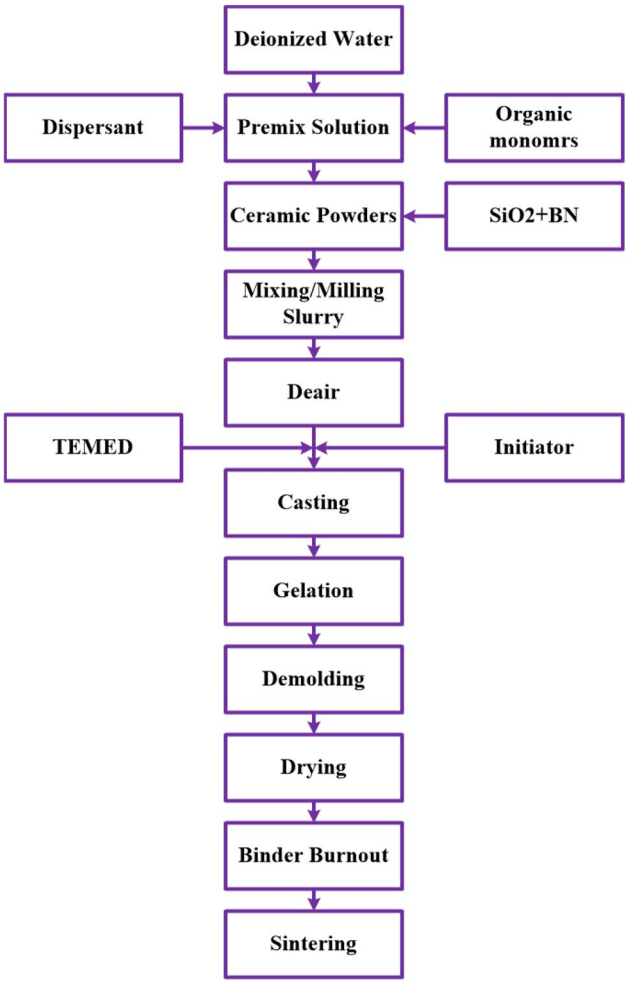

Fig. 1 A detailed flowchart of gelcasting process of concern ceramic composite

Fig. 2 Sintered samples of SiO_2–BN

4 Characterization

4.1 Flexural strength

Flexural strength (modulus of rupture) is defined as "the ability of the material to withstand bending forces applied perpendicular to its longitudinal axis". The FS was determined by the 3-point flexural process as shown in Fig. 3 with a span of 40 mm and at a crosshead speed of 0.5 mm/min using a universal testing machine as per ASTM-C1161-02C (2006) and is determined as given in Eq. 1

$$\sigma_f = \frac{3PL}{2bh^2}, \tag{1}$$

where P = fracture load, L = length of support span, b = width of the sample, and h = height of the sample.

4.2 Bulk density and apparent porosity

Bulk density is defined as "the ratio of mass to volume that includes the cavities in a porous material"

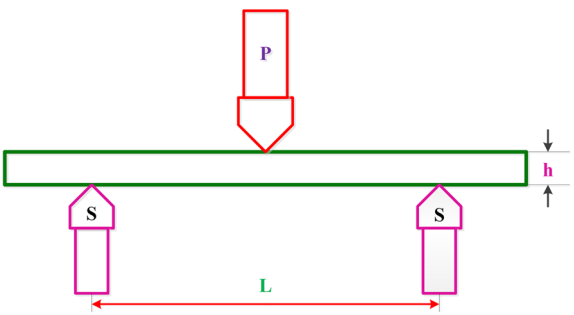

Fig. 3 Schematic of three-point bending

$$BD = \frac{DW}{SW_1 - SW_2} X\rho. \quad (2)$$

Apparent porosity is defined as "the ratio of open pore volume to total volume"

$$AP = \frac{SW_1 - DW}{SW_1 - SW_2} X\ 100, \quad (3)$$

where BD = bulk density, AP = apparent porosity, DW = dry weight, SW_1 = soaked weight, SW_2 = suspended weight, and ρ = density of kerosene oil = 0.78 gm/cc.

Bulk density and apparent porosity of ceramic bodies were determined by Archimedes principle as per ASTM C373-88(2006) using kerosene as solvent. The specimens were cut into 20 × 20 × 8 mm in size.

Archimedes principle affirms that "when an object is partially or fully immersed in a fluid it experiences an upward force that is equal to the weight of the fluid displaced by it".

4.3 Dielectric constant and loss tangent

Dielectric constant is defined as "a quantity measuring the ability of a substance to store electrical energy in an electric field".

The dielectric constant can be calculated by Eq. 4 by measuring the capacitance

$$K = \varepsilon_r^{'} = \frac{cd}{A} = \frac{\varepsilon}{\varepsilon_0}, \quad (4)$$

where K is the dielectric constant; ε_r' is relative permittivity, c is the capacitance; d is the thickness of the specimen; A is the area of the cross-sectional surface; ε is permittivity of the medium; ε_0 is permittivity of free space or vacuum.

4.4 Design of experiments

Response surface methodology consists of mathematical and statistical techniques utilized in the development of ample functional relationships among responses and process parameters. Analysis of any response of a system greatly depends on how well the experiments are designed, conducted, and measured. Therefore, conducting experiments and measuring the responses are crucial parts of any investigation. In the present study, face-centered central composite designs of RSM with 6 center points have been utilized in the test plan. The detailed experimental plan involving a number of experiments has been given in this chapter. Design Expert 9.0 software is used in the present work for RSM analysis. The measured and calculated responses FS, Por., and DE are tabulated after conducting the experiments.

Table 1 Process parameters

Variables	Units	Level 1 (− 1)	Level 2 (0)	Level 3 (1)
SL	Vol %	42	46	50
BN content	Wt %	5	10	15
MC	Wt %	10	12.5	15
RM	–	3	5	7

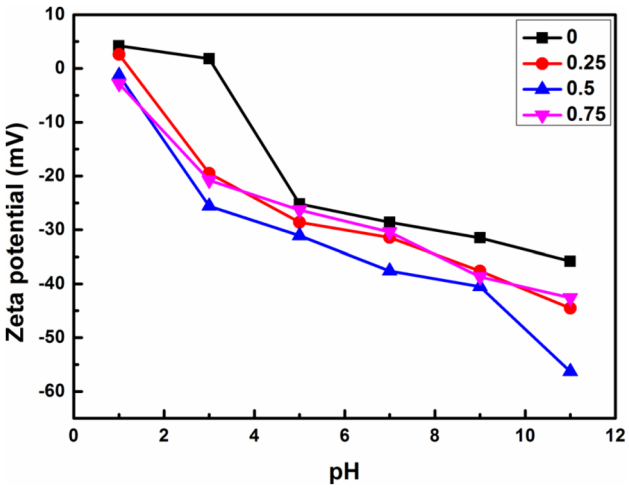

Fig. 4 Zeta potential of SiO_2–BN slurries with dispersant Darvan 821A

4.5 Experimental plan

After thorough trial experiments, the levels of solid loading (SL), Boron Nitride (BN) content, monomer content (MC), and ratio of monomers (RM) have been fixed and the levels are represented in Table 1.

A total of 30 experiments are conducted for preparation of SiO_2–BN ceramic composites including 6 center points.

5 Results and discussion

5.1 Zeta potential and pH value

The zeta potential (ZP) of SiO_2–BN slurries is studied by varying the dispersant (Darvan 821A) in the range of 0–0.75 wt% as a function of pH value and is depicted in Fig. 4. The ZP of SiO_2–BN slurry without dispersant is found to be varied from 4.2 mV at pH 1 to − 35.8 mV at pH 11. It is found that the isoelectric point (IEP) is at pH 3.1 and the absolute value of ZP increases as pH value increases. It is also observed that addition of 0.5 wt% Darvan 821A gives the maximum value of ZP which is about − 56.3 mV at pH 11, which is most suitable for obtaining well-dispersed

SiO_2–BN slurries. The other dispersant levels having good ZP other than 0.5 wt% Darvan 821A are 0.25 wt% Darvan 821A and 0.75 wt% Darvan 821A. The corresponding ZP values are − 44.5 mV and − 42.6 mV at pH 11, respectively. The ZP of the remaining slurries are found to be lower and hence not considered.

The pH value of slurry also plays a significant role on the rheological characteristics. It is found that high absolute ZP value is got by increasing the pH value of the slurry which increases the dispersibility of the slurry. The formation of hydroxide layer on the surface of SiO_2 particles is eliminated by the addition of BN particles.

5.2 Solid loading

Dense ceramics with high quality can be created by high solid loading in green bodies. Green Ceramic bodies with low solid loading suffer excessive shrinkage during binder burn-out, and with high solid loading, viscosity of the suspension increases. The optimum solid loading can be obtained by rotational rheometer [22]. Higher SL of SiO_2–BN slurry is necessary to enhance the mechanical properties of gelcast parts. The SL of the slurries are varied from 42 to 50 vol%, in which BN content varies from 5 to 15 wt%, and remaining is SiO_2. As the SL increases, the viscosity also increases making the slurry difficult to pour into mold for casting. This may be due to agglomeration at higher SL. The variation of viscosity as a function of the shear rate ranging from 0.1 to 100 s^{-1} for slurries of 50 vol% SL and with BN content varying from 5 to 15 wt% is shown in Fig. 5. It is found that there is an increase in viscosity from 0.398 to 0.53 Pa.s with an increase in BN content from 5 to 15 wt% and the gel exhibits shear-thinning behavior. Hence, slurry with 50 vol% SL and 15 wt% BN content is appropriate for casting into the mold.

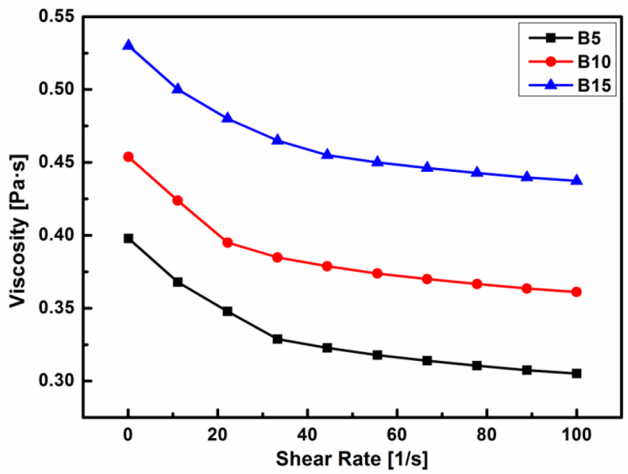

Fig. 5 Variation of the viscosity of slurry at various SL

5.3 X-ray diffraction analysis and microstructure

X-ray diffraction patterns of SiO_2–BN ceramic composite sintered at different temperatures are shown in Fig. 6. X-ray diffraction analysis is done both on raw SiO_2–BN ceramics and ceramic composite sintered at 1250 °C. It can be seen that at 1250 °C, SiO_2 is transformed into cristobalite phase. The microstructure of sintered SiO_2–BN ceramic composite is shown in Fig. 7. It is found that the pores are reduced in the SiO_2–BN ceramic composite.

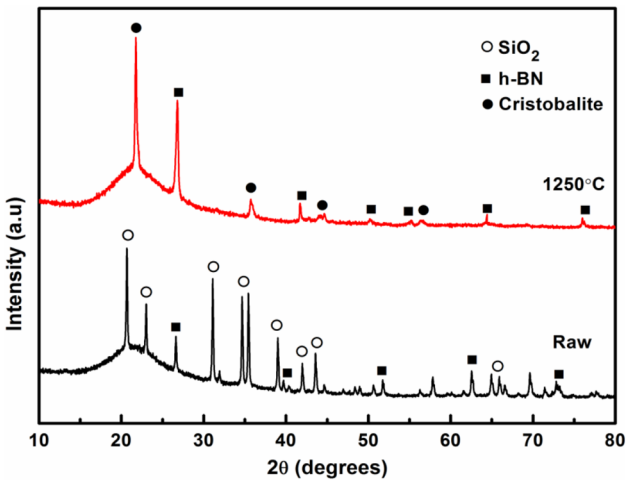

Fig. 6 XRD patterns of SiO_2–BN ceramic composite

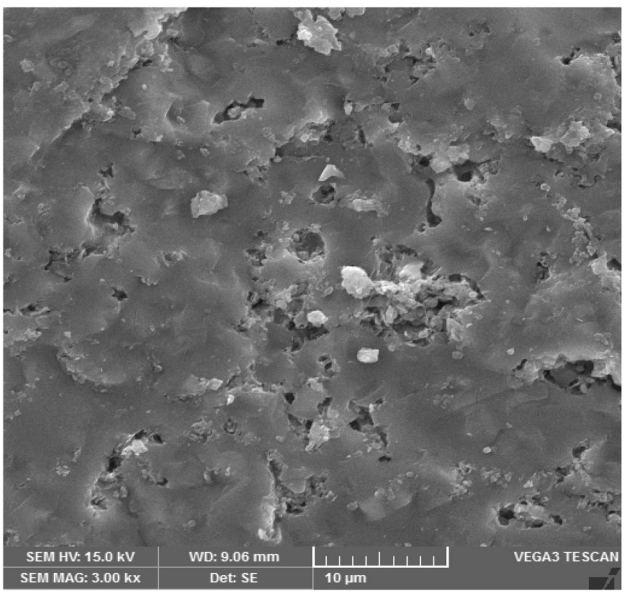

Fig. 7 SEM micrograph of sintered SiO_2–BN ceramic composite

5.4 Regression model for flexural strength

A regression model for FS of SiO_2–BN ceramic composite is fitted using the experimental results. ANOVA has been used on the test data for FS and the ANOVA results are represented in Table 2.

Here, A is SL, B is BN content, C is MC, and D is RM.

From the results, it has been found that SL, BN, and RM are important model terms, and the responses of each are shown in Fig. 8(a–c), respectively. The regression model developed for FS is given in Eq. 5, in the coded form

$$FS = 63.16 + 13.19A + 3.90B + 1.13C + 1.77D - 1.15AB - 0.76BC - 2.25A^2 - 2.17D^2. \quad (5)$$

From Fig. 8 (a) and (b), it is found that FS increases with SL and BN content. Micro-cracks occur in green bodies when the SL is less. This may be due to the increase of drying and sintering shrinkages as the space between any two particles in the slurry is huge. During sintering, the density of the composite decreases at a lower SL and BN content. Therefore, the FS of porous SiO_2–BN -sintered ceramic composite is low at lower SL and increases with the SL. In Fig. 8 (c), it can be observed that the FS increases as the RM increase from 3 to 5. This increase is due to the higher binding effect between the ceramic particles that lead to higher density in the ceramic composite. Furthermore, the FS decreases as the RM increases from 5 to 7; due to the excessive binding effect, agglomeration of ceramic particles takes place followed by the formation of micro cracks.

5.5 Regression model for porosity

A regression model for the Por. of SiO_2–BN ceramic composite is fitted using the experimental results. ANOVA has been used on the test data for Por. and the ANOVA results are presented in Table 3.

From the above results, it has been found that SL, MC, RM, interaction of SL and BN, interaction of SL and MC, interaction of SL and RM, and interaction of BN and MC, SL^2, BN^2, MC^2, and RM^2 are important model terms, and the response of each are shown in Fig. 9(a–h). The mathematical model developed for Por. was given in Eq. 6, in the coded form

$$\text{Por.} = 21.02 - 2.20A + 0.19B + 0.5C - 1.06D - 0.29AB + 0.37AC - 0.45AD - 0.57BC - 0.12BD - 0.18CD - 1.53A^2 - B^2 + 0.7C^2 + 1.17D^2. \quad (6)$$

The Por. of sintered body decreases with the increase of SL, as shown in Fig. 9 (a). As the SL increases, the ceramic particles are tightly packed. This densifies the ceramic composite reducing the pores in the composite. From Fig. 9 (b), it is found that BN content has an important influence on the Por. As the BN content increases, there is a rise in the Por. and then declines on further addition of BN powder. The rise in the Por. is due to the loose packing of BN particles in SiO_2 ceramics. As the content of BN powder increases, the pores in the composite are reduced that increases the density of the composite causing the lower Por.

The Por. of sintered sample increases with the increase of MC as seen in Fig. 9 (c). The pores of sintered body largely

Table 2 ANOVA for FS

Source	Sum of squares	df	Mean square	*F* value	*p* Value Prob > *F*	Percentage contribution
Model	3541.214	8	258.9827	44.74187	< 0.0001	97.607
A-SL	3132.890	1	3132.889	541.2381	< 0.0001	86.352
B-BN	273.156	1	273.1564	47.19051	< 0.0001	7.529
C-MC	23.165	1	23.16536	4.002048	0.0639	0.639
D-RM	56.463	1	56.46302	9.754555	0.0070	1.556
AB	21.091	1	21.09106	3.643692	0.0756	0.581
BC	9.136	1	9.135506	1.578251	0.2282	0.252
A^2	13.086	1	13.08581	2.260706	0.1535	0.361
D^2	12.227	1	12.22698	2.112333	0.1667	0.337
Residual	86.826	21	5.788375			2.393
Cor total	3628.039	29				100.00

R^2: 97.66%

Adjusted R^2: 95.47%

Predicted R^2: 93.02%

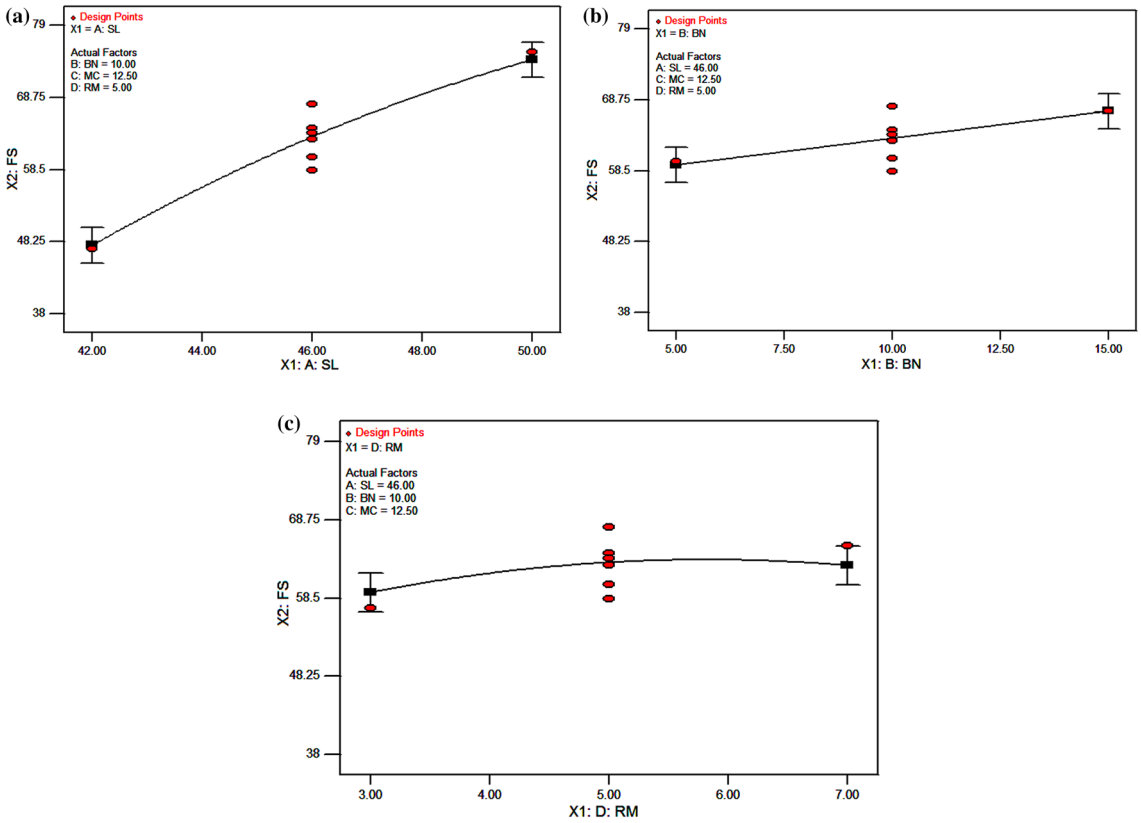

Fig. 8 Effect of process parameters on flexural strength

Table 3 ANOVA for Por

Source	Sum of squares	df	Mean square	*F* value	*p* Value Prob > *F*	Percentage contribution
Model	118.481	14	6.856034	38.8316	< 0.0001	98.387
A-SL	82.112	1	86.81227	491.6924	< 0.0001	68.186
B-BN	0.076	1	0.07605	0.430736	0.5251	0.063
C-MC	4.500	1	4.5	25.48736	0.0004	3.737
D-RM	2.226	1	2.22605	12.60803	0.0045	1.849
AB	1.369	1	1.3689	7.753255	0.0178	1.137
AC	2.205	1	2.205225	12.49008	0.0047	1.831
AD	3.186	1	3.186225	18.04633	0.0014	2.646
BC	5.198	1	5.1984	29.443	0.0002	4.317
BD	0.250	1	0.25	1.415964	0.2591	0.208
CD	0.426	1	0.525625	2.977065	0.1124	0.353
A^2	5.048	1	6.047685	34.25323	0.0001	4.192
B^2	2.580	1	2.579558	14.61025	0.0028	2.142
C^2	1.259	1	1.259384	7.132972	0.0218	1.046
D^2	8.046	1	8.045612	45.5692	< 0.0001	6.681
Residual	1.942	15	0.176558			1.613
Cor total	120.423	29				100.00

R^2: 98.45%

Adjusted R^2: 95.91%

Predicted R^2: 80.45%

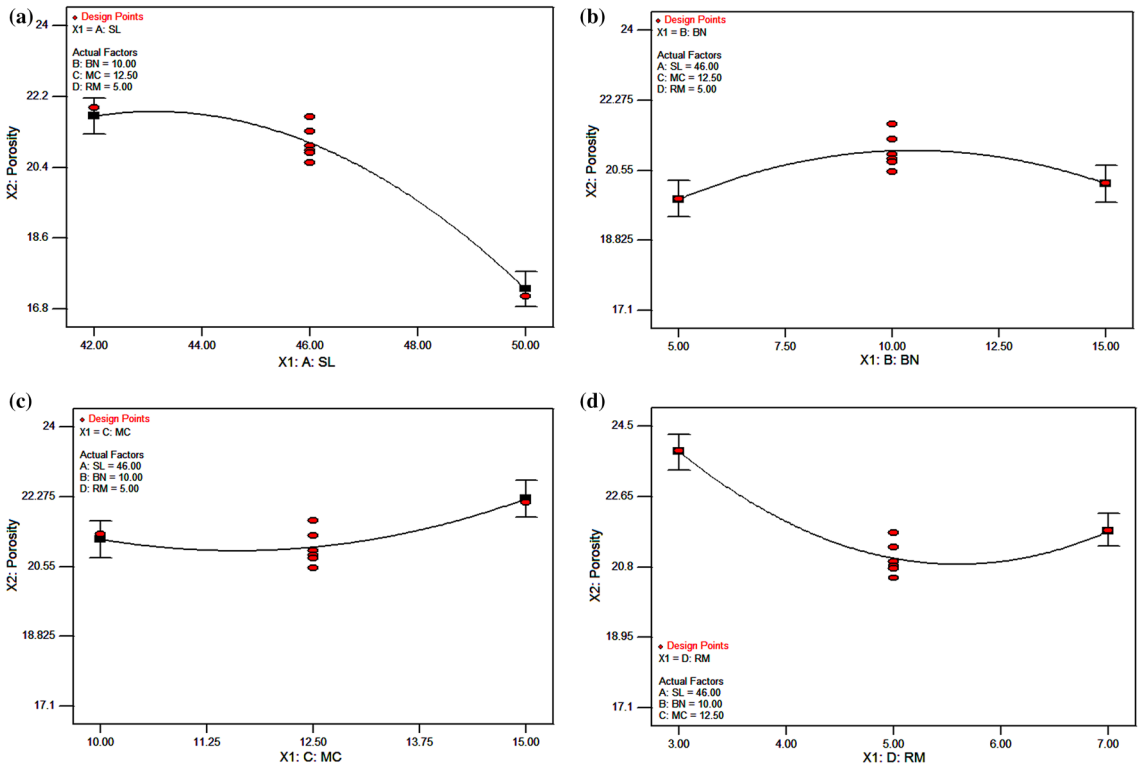

Fig. 9 Effect of process parameters on porosity

initiate from the left-over micro-space of the organic polymers in the green sample during organic binder burn-out. The distribution and intensity of pores depend on the MC. In Fig. 9 (d), the Por. decreases initially with the increase of RM and then rises on further increase in the RM. The increase in the RM to cross-linker sometimes initiates micro-crack propagation that causes higher Por.

5.6 Regression model for dielectric constant

A regression model for DE of SiO_2–BN ceramic composite is fitted using the experimental results. ANOVA has been used on the test data for DE and the ANOVA results are presented in Table 4.

From the above results, it has been found that SL, MC, RM, SL^2, BN^2, MC^2, RM^2, interactions of SL and MC, and interactions of SL and RM are important model terms, and the response of each are shown in Fig. 10(a–f). The regression model developed for DE was given in Eq. 7, in the coded form

$$\begin{aligned} DE = {} & 4.62 + 0.35A - 0.019B - 0.033C \\ & + 5.556 \times 10^{-3} D - 0.02AB - 0.077AC \\ & + 0.061AD + 0.038BC + 0.24A^2 \\ & + 0.23B^2 - 0.18C^2 - 0.25D^2. \end{aligned} \quad (7)$$

As shown in Fig. 10 (a), with the increase in SL, density of SiO_2–BN ceramic composite increases that will lead to the reduction of pores that causes the increase of DE. It can be seen in Fig. 10 (b) that the DE initially decreases from 5 to 10 wt% of BN content due to the increase in the surface area of pores. On further increasing the BN content from 10 to 15 wt%, there is a rise in the DE due to the increase in the density of the ceramic composite that lowers the transfer of electromagnetic waves through it. In Fig. 10 (c), as the MC increases, the DE increases and reaches a maximum point and then decreases. The increase in MC decreases the density of sintered ceramic composite due to the formation of large pores during binder burn-out. Thus, an increase in the MC will lower the density and dielectric properties of ceramics. Few of the pores may be replaced by the BN ceramic particles causing an increase in the DE at MC of 12.5 wt%.

In Fig. 10 (d), it can be observed that the DE increases as the RM increases from 3 to 5. This increase is due to the higher binding effect between the ceramic particles that leads to low pores. Furthermore, the DE decreases as the RM increases from 5 to 7; due to the excessive binding effect, agglomeration of ceramic particles takes place followed by the formation of micro cracks.

Table 4 ANOVA for DE

Source	Sum of squares	df	Mean square	*F* value	*p* Value Prob > *F*	Percentage contribution
Model	2.788	12	0.23396	23.59431	< 0.0001	94.299
A-SL	2.094	1	2.18405	220.2558	< 0.0001	70.826
B-BN	0.007	1	0.006806	0.686323	0.4189	0.230
C-MC	0.019	1	0.019339	1.950277	0.1805	0.654
D-RM	0.001	1	0.000556	0.056026	0.8157	0.019
AB	0.006	1	0.0064	0.645423	0.4328	0.216
AC	0.096	1	0.0961	9.691437	0.0063	3.250
AD	0.050	1	0.060025	6.053366	0.0249	1.692
BC	0.023	1	0.0225	2.269067	0.1503	0.761
A^2	0.146	1	0.146089	14.73275	0.0013	4.941
B^2	0.134	1	0.134044	13.518	0.0019	4.534
C^2	0.081	1	0.086335	8.706657	0.0089	2.751
D^2	0.131	1	0.158766	16.0111	0.0009	4.423
Residual	0.169	17	0.009916			5.701
Cor total	2.957	29				100.00

R^2: 94.34%

Adjusted R^2: 90.34%

Predicted R^2: 80.6%

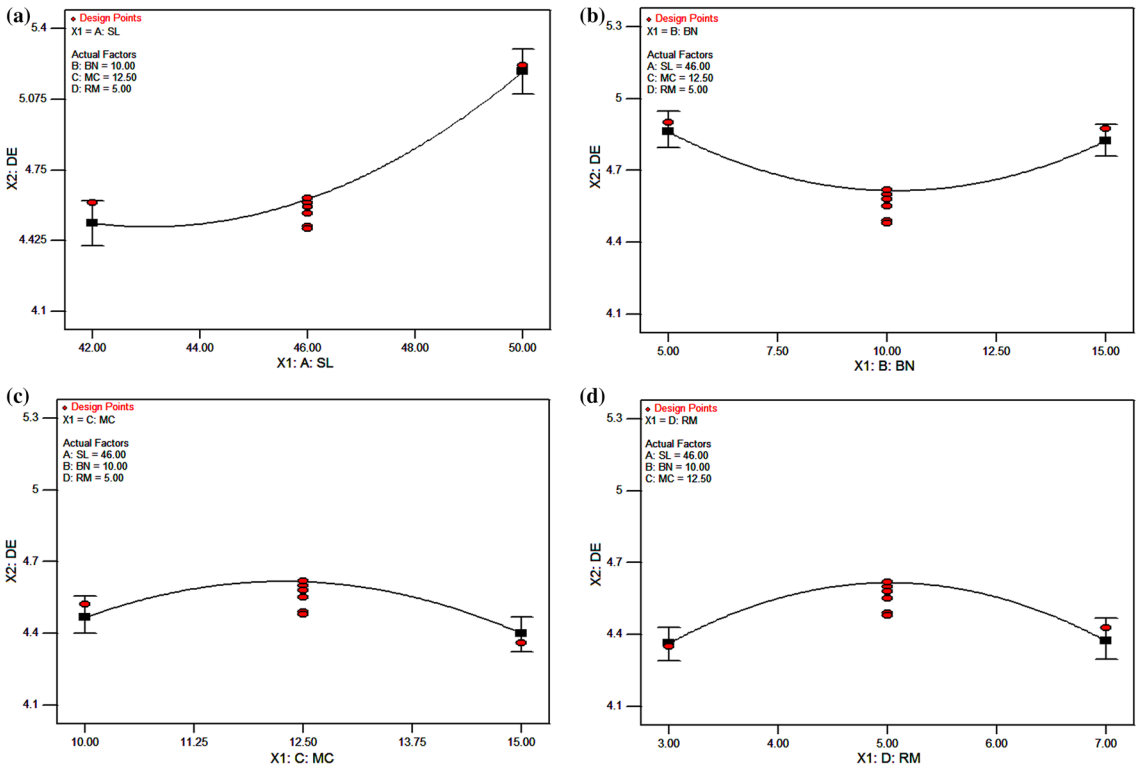

Fig. 10 Effect of process parameters on dielectric constant

Table 5 The range of input parameters and output

Name	Goal	Lower limit	Upper limit
A-SL (vol %)	Maximize	42	50
B-BN content (wt %)	In range	5	15
C-MC (wt %)	Is in range	10	15
D-RM	Is in range	3	7
FS (MPa)	Maximize	38.11	78.19
Por. (%)	Maximize	17.12	23.99
DE	Minimize	4.12	5.23

5.7 Multi-objective optimization using desirability function

Multi-objective optimization using desirability function was carried out in combination with RSM to surmount the difficulty of inconsistent responses of single response optimization. The range and goals of input variables, i.e., SL, MC, RM, and BN contents and the responses, i.e., FS, Por., and DE, are given in Table 5.

The aim of optimization is to evaluate the best combinational set of inputs for maximization of flexural strength and porosity, and minimization of dielectric constant. This is indicated by the desirability of RSM analysis. The optimum value of responses is to be chosen for maximum desirability index for various sets of inputs. A set of ten optimal solutions is derived and tabulated in Table 6 for the particular set of input range (Table 5). The desirability of output responses, i.e., FS, Por., and DE, is shown in Fig. 11 as ramp graph. The desirability of each parameter and each response and combined parameters are shown in Fig. 12 as a bar graph. The overall desirability of the responses is found to be 0.812.

5.8 Confirmation tests

The values of responses, i.e., flexural strength, porosity, and dielectric constant, obtained by experimental runs are compared with predicted regression models for flexural strength, porosity, and dielectric constant for SiO_2–BN ceramic composite.

The error between experimental and predicted values is predicted in Table 7 for all responses. It is found a maximum error of ± 3.45% in flexural strength, ± 3.06% in porosity, and ± 3.13% in dielectric constant existing. Hence, it can be declared that the predicted models are confirming with experimental values. Hence, the tests are confirmed and recommended that the models are accurate.

6 Conclusions

The following conclusions were drawn from the present work.

- Fused silica (SiO_2)-based ceramic composites SiO_2–BN has been successfully produced using gelcasting method.
- The rheological behavior of the SiO_2 suspensions including SiO_2–BN by varying dispersant content, pH value, and solid loading has been thoroughly studied, and useful ranges of SL, MC, RM, and BN contents were decided based on trial experiments and they are as follows.

  I. Solid loading: 68–72 vol% for SiO_2 ceramics and 42–50 vol% for SiO_2–BN ceramic composites
  II. Monomer content: 10–15 wt%
  III. Ratio of monomers: 3–7
  IV. BN content: 5–15 wt%.

- Darvan 821A is recommended as a dispersant and a dosage of 0.5 wt% showed better results over other dispersants in the suspension of ceramic particles as 0.5 wt%

Table 6 Set of optimal solutions for SiO_2–BN ceramic composite

Number	SL	BN	MC	RM	FS	Por	DE	Desirability
1	47.97	9.68	15	3	66.301	23.958	4.307	0.812
2	47.95	9.75	15	3	66.301	23.961	4.305	0.812
3	47.96	9.49	15	3	66.184	23.988	4.306	0.812
4	48.06	9.89	15	3	66.643	23.841	4.317	0.812
5	48.17	9.41	15	3	66.714	23.782	4.330	0.811
6	47.92	9.9	15	3.01	66.313	23.956	4.304	0.811
7	47.95	8.8	15	3.02	65.901	23.989	4.318	0.807
8	47.72	11.62	15	3	66.598	23.822	4.314	0.800
9	47.01	10.55	15	3	64.085	24.626	4.220	0.779
10	48.23	13.52	15	3	68.799	22.630	4.472	0.756

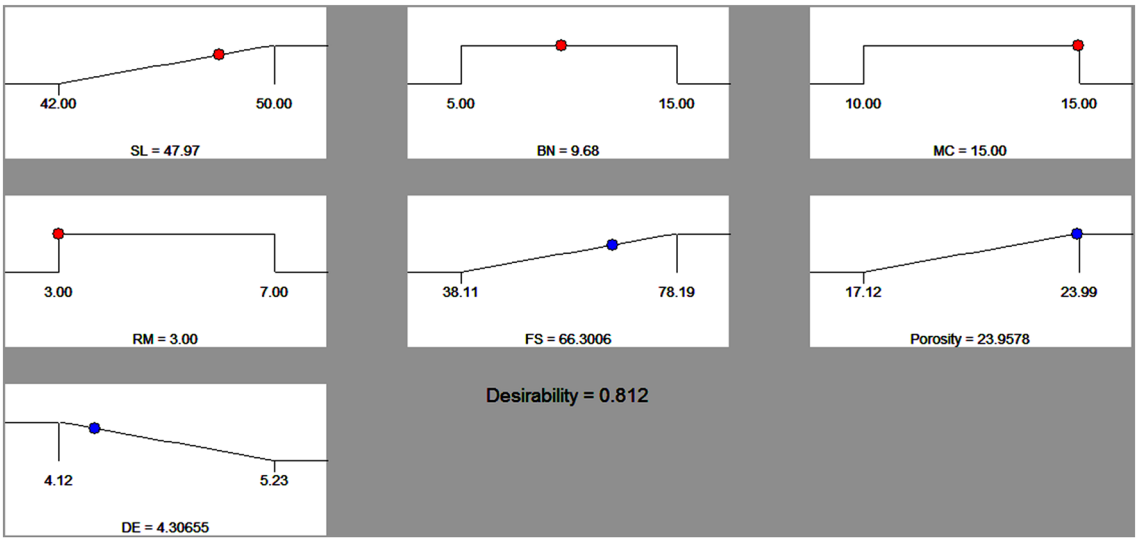

Fig. 11 Ramp graphs of desirability function for SiO_2–BN ceramic composite

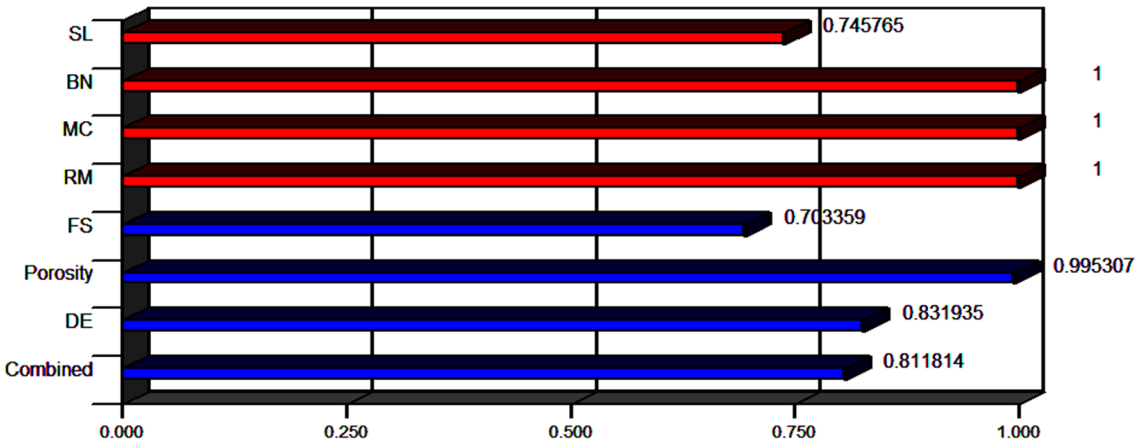

Fig. 12 Bar graphs of desirability function for SiO_2–BN ceramic composite

Darvan 821A gives the maximum zeta potential value for all SiO_2 suspensions.

- Tests for FS, Por., and DE were conducted for all the samples of SiO_2–BN.
- The regression models for the analysis of responses such as FS, Por., and DE are developed, and the effects of the process parameters on these responses are studied.
- The optimum process parameters for maximum FS, maximum Por., and minimum DE were evaluated using RSM coupled with desirability function to optimize multiple responses.
- The values of responses, i.e., FS, Por., and DE, obtained by experimental runs are compared with predicted regression models for FS, Por., and DE for SiO_2–BN ceramic composites.
- The above results can be applied in the fabrication of radomes and wave transparent applications.

Table 7 Error between experimental and predicted values

Run order	SL (vol %)	BN (wt %)	MC (wt %)	RM	Flexural strength (MPa)			Porosity (%)			Dielectric constant (K)		
					Expt.	Pred.	Error	Expt.	Pred.	Error	Expt.	Pred.	Error
1	46	10	15	5	66.28	64.55	2.60	22.13	22.22	− 0.42	4.34	4.40	− 1.39
2	46	10	12.5	3	57.43	59.22	− 3.11	23.86	23.84	0.08	4.35	4.36	− 0.28
3	50	15	10	3	71.65	72.57	− 1.28	19.08	18.93	0.76	4.98	5.01	− 0.50
4	46	10	10	5	61.13	62.29	− 1.89	21.35	21.22	0.60	4.61	4.47	3.13
5	46	10	12.5	5	62.77	63.16	− 0.62	21.31	21.02	1.34	4.58	4.62	− 0.77
6	46	10	12.5	7	64.98	62.76	3.42	21.75	21.73	0.08	4.51	4.37	3.03
7	50	5	10	3	66.29	65.92	0.57	17.46	17.36	0.57	5.12	5.08	0.80
8	46	5	12.5	5	59.84	59.30	0.90	19.85	19.83	0.09	4.9	4.86	0.77
9	50	5	10	7	69.18	69.64	− 0.67	17.83	18.23	− 2.26	5.1	5.21	− 2.21
10	42	15	10	7	51.19	52.17	− 1.92	23.89	24.11	− 0.94	4.12	4.12	− 0.11
11	50	10	12.5	5	75.18	74.11	1.43	17.12	17.30	− 1.06	5.23	5.20	0.55
12	42	15	15	7	52.51	53.13	− 1.18	23.71	23.54	0.72	4.21	4.29	− 1.88
13	50	5	15	3	70.58	69.49	1.54	21.22	21.27	− 0.26	4.82	4.78	0.76
14	50	15	15	7	76.45	77.22	− 1.01	17.8	17.95	− 0.83	5	4.99	0.14
15	46	10	12.5	5	64.37	63.16	1.88	20.83	21.02	− 0.93	4.62	4.62	0.10

References

1. H. Song, J. Dan, X. Chen, J. Xiao, J. Xu, Experimental investigation of machinability in laser-assisted machining of fused silica. Int J Adv Manuf Technol **97**, 267–278 (2018)
2. K.K. Kandi, G. Punugupati, S.K. Pal, S.P. Rao Chilakalapalli, Effect of monomers content and their ratio on gelcasting of fused silica ceramics. Trans Indian Ceram Soc **75**(3), 185–188 (2016)
3. G. Punugupati, P.S.C. Bose, G. Raghavendra, C.S.P. Rao, Influence of solid loading and ratio of monomers on mechanical and dielectric properties of hybrid ceramic composites. SILICON **11**(6), 2701–2710 (2019)
4. H. Du, Y. Li, C. Cao, Effect of temperature on dielectric properties of Si_3N_4/SiO_2 composite and silica ceramic. J Alloy Compd **503**(1), L9–L13 (2010)
5. W. Wan, J. Yang, Y. Feng, W. Bu, T. Qiu, Effect of trace alumina on mechanical, dielectric, and ablation properties of fused silica ceramics. J Alloy Compd **675**, 64–72 (2016)
6. B. Chen, X. Liu, X. Zhao, Z. Wang, L. Wang, W. Jiang, J. Li, Preparation and properties of reduced graphene oxide/fused silica composites. Carbon **77**, 66–75 (2014)
7. S. Abbas, S. Maleksaeedi, E. Kolos, A.J. Ruys, Processing and properties of zirconia-toughened alumina prepared by Gelcasting. Materials **8**(7), 4344–4362 (2015)
8. J. Eichler, C. Lesniak, Boron nitride (BN) and BN composites for high-temperature applications. J Eur Ceram Soc **28**, 1105–1109 (2008)
9. B. Yuan, J.X. Liu, G.J. Zhang, Y.M. Kan, P.L. Wang, Silicon nitride/boron nitride ceramic composites fabricated by reactive pressureless sintering. Ceram Int **35**, 2155–2159 (2009)
10. W. Dong, C.A. Wang, L. Yu, S.X. Ouyang, Effect of sintering additive content on mechanical and dielectric properties of porous Si_3N_4/BN composite ceramics. J Chin Ceram Soc **40**, 851–855 (2012)
11. G. Wen, G.L. Wua, T.Q. Lei, Y. Zhou, Z.X. Guob, Co-enhanced SiO2-BN ceramics for high-temperature dielectric applications. J Eur Ceram Soc **20**, 1923–1928 (2000)
12. D. Jia, L. Zhou, Z. Yang, X. Duan, Y. Zhou, Effect of preforming process and starting fused SiO2 particle size on microstructure and mechanical properties of pressurelessly sintered BNp/SiO2 ceramic composites. J Am Ceram Soc **94**, 3552–3560 (2011)
13. W. Dong, C.A. Wang, L. Yu, S.X. Ouyang, Preparation and properties of porous Si_3N_4-SiO_2-BN composite ceramics. Key Eng Mater **512–515**, 828–831 (2012)
14. M. Du, J.Q. Bi, W.L. Wang, X.L. Sun, N.N. Long, Microstructure and properties of SiO2 matrix reinforced by BN nanotubes and nanoparticles. J. Alloy Compd **509**, 9996–10002 (2011)
15. H. Zhai, H. Cai, X. Yang, J. Li, G. Guo, C. Cao, Preparation and properties of BN-SiO_2 composite ceramics. Key Eng Mater **336–338**, 1426–1428 (2007)
16. D.G. Montgomery, *Design and analysis of experiments*, 8th edn. (Wiley, New York, 2012)
17. G.E.P. Box, N.R. Draper, *Empirical model building and response surfaces* (Wiley, New York, 1987)
18. G. Punugupati, P.S.C. Bose, G. Raghavendra, C.S.P. Rao, Response surface modeling and optimization of Gelcast fused silica micro hybrid ceramic composites. SILICON **12**(7), 1513–1528 (2020)
19. C. Song, X. Li, L. Wang, W. Shi, Fabrication, characterization and response surface method (RSM) optimization for tetracycline photodegration by Bi 3.84 W 01.6 O 6.24-graphene oxide (BWO-GO). Sci Rep **6**(1), 1–12 (2016)
20. J. Li, J. Peng, S. Guo, L. Zhang, Application of response surface methodology (RSM) for optimization of sintering process for the preparation of magnesia partially stabilized zirconia (Mg-PSZ) using natural baddeleyite as starting material. Ceram Int **39**(1), 197–202 (2013)
21. F. Xiangli, W. Wei, Y. Chen, W. Jin, N. Xu, Optimization of preparation conditions for polydimethylsiloxane (PDMS)/ceramic composite pervaporation membranes using response surface methodology. J Membr Sci **311**(1–2), 23–33 (2008)
22. C.-J. Bae, A. Ramachandran, K. Chung, S. Park, Ceramic stereolithography: additive manufacturing for 3D complex ceramic structures. J Korean Ceram Soc **54**(6), 470–477 (2017)